# Paramagnetic gold nanostructures for dual modal bioimaging and phototherapy of cancer cells†

**Yong Taik Lim, Mi Young Cho, Bang Sil Choi, Jung Min Lee and Bong Hyun Chung***

*Received (in Cambridge, UK) 17th June 2008, Accepted 29th July 2008*
*First published as an Advance Article on the web 29th August 2008*
**DOI: 10.1039/b810240f**

**Paramagnetic gold nanostructures were synthesized by combining the paramagnetism of gadolinium with the plasmonic properties of gold nanoparticles and used for dual modal (MRI and optical) imaging and phototherapy of breast cancer cells.**

Multifunctional nanomaterials having both magnetic and optical properties are expected to play important roles in the diagnosis and treatment of cancer.[1] Recently, hybrid nanoparticles combining the plasmonic character of gold nanoparticles and the magnetic properties of iron oxide nanoparticles have been developed for the biomedical imaging and therapy of cancer cells.[2] In previous research, gold nanoparticles have emerged as an attractive therapeutic moiety for cancer cells because of their strong light-absorption properties, known as surface plasmon resonance (SPR).[3] Superparamagnetic iron oxide nanoparticles have been extensively studied for use as magnetic resonance imaging (MRI) contrast agents because in the presence of an external magnetic field, a magnetic field is induced within these nanoparticles that polarizes the spins of neighboring water protons, resulting in enhanced contrast in the final image.[4] However, the significant drawbacks of superparamagnetic iron oxide nanoparticles as MRI contrast agents are magnetic susceptibility artifacts and negative contrast effects. Because the susceptibility artifacts distort the background image and the distorted image is often interpreted as a signal from bleeding or calcification, the error can result in a misleading clinical diagnosis from T2-weighted MRI.[5]

To overcome the above-mentioned drawbacks and to extend the applications of multifunctional gold nanostructures, we have designed paramagnetic gold nanostructures for molecular imaging and therapy of cancer cells. In this study, we report the synthesis of paramagnetic gold nanostructures with both MRI- and scattering-based optical imaging modalities as well as a photonics-based cancer therapeutic effect (Fig. 1). Paramagnetic compounds generate signal contrast by enhancing the longitudinal relaxation rates of water protons in the surrounding tissue.[6] The relaxation time can be manipulated using paramagnetic contrast agents such as gadolinium diethylenetriaminepentaacetic acid (Gd-DTPA) that efficiently shorten T1, resulting in enhanced signals in T1-weighted images. In this context, gold nanostructures were synthetically designed for their optical resonance (absorption and scattering) peaks to be located around the near-infrared (NIR) wavelength region which is optimal for *in vivo* optical imaging and therapy.[7] The paramagnetic gold nanostructures were used as cellular probes to image cancer cells using a clinical MRI scanner and dark-field scattering microscopy. Cancer cells targeted with a paramagnetic gold nanostructure were finally destroyed by the photothermal effect induced by NIR irradiation.

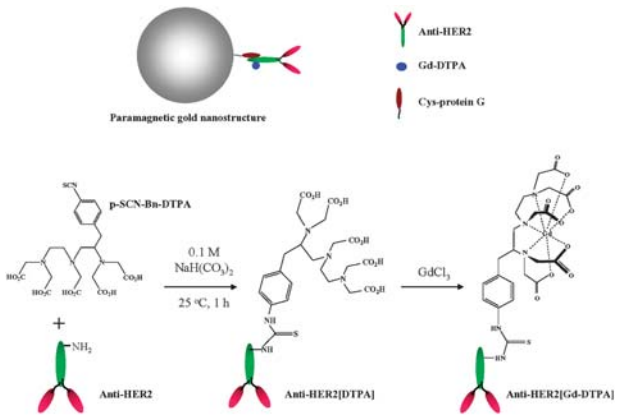


**Fig. 1** Schematic illustration of the structure and synthesis of paramagnetic gold nanostructures. After anti-HER2 was chemically conjugated with Gd-DTPA, the combination was attached to the surfaces of gold nanoparticles coated with protein G.

A schematic representation of the synthesis of paramagnetic hollow gold nanoparticles is shown in Fig. 1. The experimental details are available in the ESI.† Anti-HER2 is a monoclonal antibody that targets epidermal growth factor receptors (EFGRs) overexpressed on the surfaces of breast cancer cells such as SKBR3.[8] For chelation of the paramagnetic compound, DTPA (*p*-SCN-Bn-DTPA) was reacted with breast cancer cell (SKBR3)-targeting antibodies (anti-HER2) using the reaction scheme shown in Fig. 1. Gd(III) ions ($GdCl_3$) were then introduced and chelated by DTPA conjugated with anti-HER2 (anti-HER2[DTPA]). After chelating $Gd^{3+}$ ions onto DTPA containing antibody, we removed unbound Gd ions by dialysis for one week. The surfaces of hollow gold nanoparticles were modified with cystein-protein G and thiol-PEG molecules.[8,9] PEG moieties were used to increase water solubility and to block nonspecific interactions, resulting in increases in both particle blood circulation time and the efficiency of particle internalization by targeted cells *in vivo*.[8] Protein G molecules were

*BioNanotechnology Research Center, Korea Research Institute of Bioscience and Biotechnology (KRIBB), P.O. Box 115, Yuseong, Daejeon 305-600, Korea. E-mail: chungbh@kribb.re.kr; Fax: (+82) 42 879 8594; Tel: (+82) 42 860 4442*

† Electronic supplementary information (ESI) available: Experimental details for synthesis and properties of materials. See DOI: 10.1039/b810240f

 

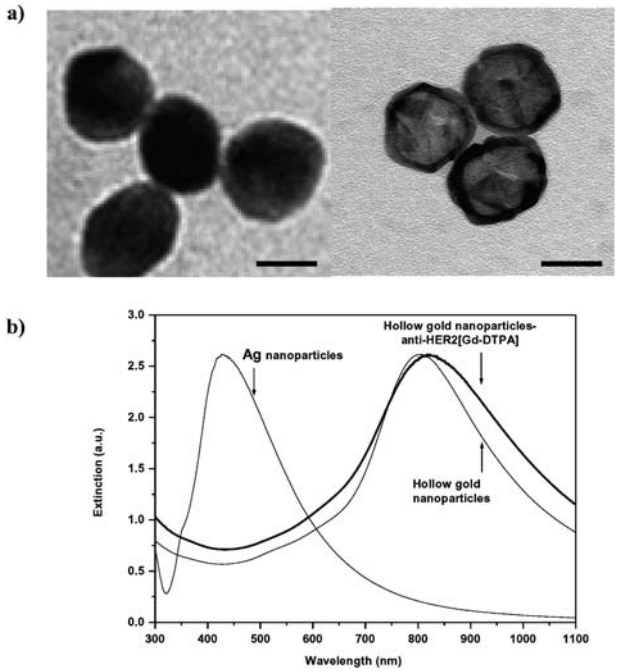


**Fig. 2** (a) Transmission electron microscope images of solid silver nanoparticles (left) and hollow-type gold nanoparticles (right). The scale bars represent 50 nm. (b) UV–Vis–NIR spectroscopy of silver nanoparticles, hollow-type gold nanoparticles, and paramagnetic gold nanoparticles.

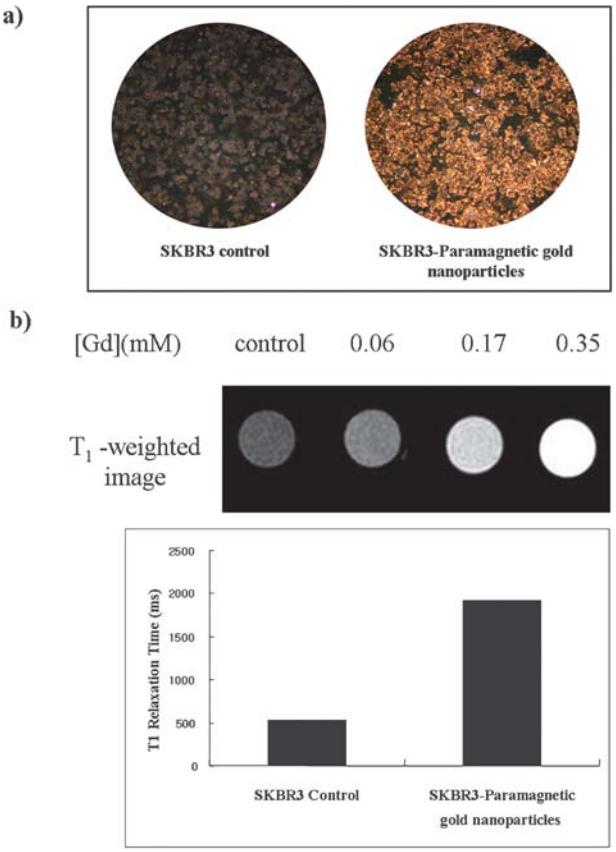


**Fig. 3** Dual modal cellular imaging of SKBR3 breast cancer cells targeted with paramagnetic gold nanoparticles conjugated with anti-HER2[Gd-DTPA]. (a) Dark-field-based scattering images and (b) magnetic resonance images of SKBR3 cells labeled with various concentrations of Gd ions (T1 relaxation time data were obtained at 0.17 mM Gd concentration).

introduced to optimize the orientation of antibodies on the surfaces of the hollow gold nanoparticles.[9] Finally, the breast cancer-targeting antibodies conjugated with Gd (anti-HER2-[Gd-DTPA]) were reacted with the protein G moieties on hollow gold nanoparticles to confer on the hollow gold nanoparticles the paramagnetic characteristics required for T1-weighted MRI.

Fig. 2a shows a TEM image of hollow gold nanoparticles synthesized *via* the replacement reaction of silver nanoparticles with chloroauric acid solutions.[10] A TEM image of low magnification is also available in the ESI.† Gold nanostructures with optical resonance peaks located around the NIR region of the spectrum are preferred because the NIR wavelength region allows high light penetration through biological tissues (both blood and soft tissue).[7] The final optical resonance peaks of the hollow gold nanoparticles were finely tuned by controlling the molar ratio of solid silver nanoparticles and chloroauric acid in reaction solutions.[10] When chloroauric acid solutions were added to solid silver nanoparticles, the optical resonance peak of the silver nanoparticles (approximately 450 nm) shifted to around the 808 nm region of the spectrum (Fig. 2b). This spectral shift indicates the structural change of silver nanoparticles into hollow gold nanoparticles. After conjugation of anti-HER2[Gd-DTPA], the UV–Vis absorption was red-shifted due to the change of environment around the gold surface. The relaxivity values for the hollow gold nanoparticles conjugated with anti-HER2-[Gd-DTPA] were analyzed and the experimental data are available in the ESI.† Briefly, the relaxivity values of $r_1$ (the slope of $1/T_1 = f$[Gd]) and $r_2$ (the slope of $1/T_2 = f$[Gd]) for paramagnetic gold nanoparticles were 23.7 $mM^{-1}$ $s^{-1}$ and 89.5 $mM^{-1}$ $s^{-1}$, respectively. It seems that Gd-DPTA is conjugated on antibody and strongly anchored by the rigid gold nanoparticles, resulting in a low tumbling rate and subsequently high relaxivity.

The targeting capacity of hollow gold nanoparticles conjugated with anti-HER2[Gd-DTPA] was investigated using the light-scattering properties of the hollow gold nanoparticles (Fig. 3a). A brightly scattered light image was observed when the hollow gold nanoparticles conjugated with anti-HER2[Gd-DTPA] were targeted, whereas no signal was observed in the control experiments performed without antibodies. Although the scattering-based imaging methods are highly promising for ultra-sensitive biological detection and single cell imaging, they cannot be directly applied to a non-invasive *in vivo* imaging system. Thus, MRI can serve as a powerful non-invasive imaging tool in both clinical and research fields because of the superior quality of MRI high-resolution images. The MR images of SKBR3 breast cancer cells targeted with various concentrations of paramagnetic hollow gold nanoparticles were obtained using a clinical MRI scanner (1.5 T, Philips) (Fig. 3b). The paramagnetic Gd(III) ions in the hollow gold nanoparticles conjugated with anti-HER2-[Gd-DTPA] were used to increase the intrinsic contrast of SKBR3 MRI by reducing the relaxation time of water protons around the SKBR3 cells, thus producing an increase in signal intensity.

When the cells targeted with paramagnetic gold nanoparticles conjugated with anti-HER2[Gd-DTPA] were

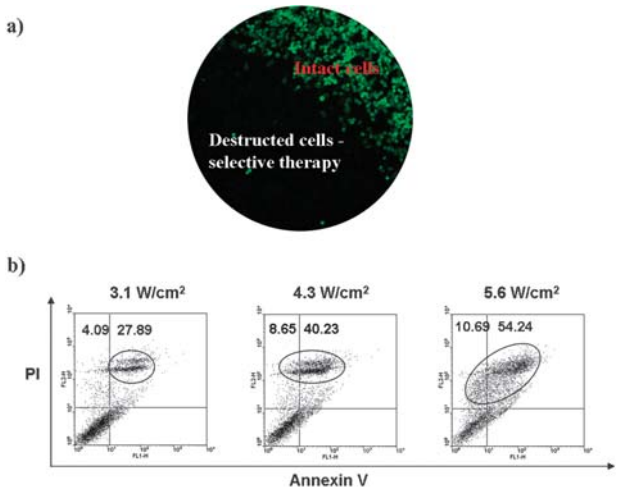


**Fig. 4** (a) Fluorescence image of SKBR3 cells stained with calcein-AM and (b) FACS analysis of death modes of SKBR3 breast cancer cells after NIR irradiation (power densities = 3.1, 4.3 and 5.6 W $cm^{-2}$) of cells targeted with paramagnetic gold nanoparticles conjugated with anti-HER2[Gd-DTPA]. The two numbers in each of the FACS data represent the percentages of each cell death mechanism: the percentages of cells suffering necrotic death (Annexin $V^-/PI^+$; left), and late apoptotic or secondary necrotic death (Annexin $V^+/PI^+$; right).

irradiated with a NIR laser at various laser power intensities, the energy absorbed by the gold nanoparticles was converted into thermal energy. The temperature of cells targeted with gold nanoparticles ranged from 45 to 75 °C, resulting in cell damage. Fig. 4a shows the destructive effect of the paramagnetic hollow gold nanoparticles on the SKBR3 cells. Photothermal destruction of SKBR3 cells was observed only where paramagnetic hollow gold nanoparticles were bound and with NIR laser irradiation (808 nm, 3.1 W $cm^{-2}$). The threshold laser power densities for the selective destruction of cancer cells were substantially lower than those reported for silica–gold core–shell type gold nanoshells (35 W $cm^{-2}$) or gold nanorods (10 W $cm^{-2}$).[3a,b] To observe the effect of NIR laser power intensity on cell death, the laser power was varied under conditions where the concentration of paramagnetic hollow gold nanoparticles was fixed (the optical density [O.D.] was 2.0 at 808 nm). The degree of apoptosis (programmed cell death) and necrosis was examined by measuring the binding of Annexin V–fluorescein and inclusion/exclusion of propidium iodide (PI) using a FACSCalibur flow cytometer. Annexin $V^-/PI^+$ and Annexin $V^+/PI^+$ events represent necrosis and late apoptosis (or secondary necrosis), respectively (Fig. 4b).

As shown in Fig. 4b, the amount of cell death increased with increasing laser power. Interestingly, cell death was dominated by late apoptosis-related or secondary necrosis-related death at varying laser power intensities. Death from necrosis increased at higher laser power (10.69% at 5.6 W $cm^{-2}$). Although hyperthermia has been under investigation as an effective and useful tool for anti-cancer therapy, the cellular and molecular pathways underlying this beneficial procedure are still poorly understood.[11] More detailed molecular-level studies on the photothermal behavior induced by light-absorbing nanoparticles, and the pathways of cell death after such treatment, are required. To our knowledge, this is the first report on the analysis of cell death mechanism (*i.e.* apoptosis or necrosis) induced by a photothermal effect generated by light-absorbing gold nanoparticles. Although, as mentioned above, more systematic studies are still required, our findings offer some clues for the development of novel strategies of cancer therapy. For example, a photonic-based cancer therapy strategy employing paramagnetic gold nanostructures could be combined with chemotherapies using various anticancer drugs to induce specific cell death.

In conclusion, we report the synthesis of paramagnetic hollow gold nanoparticles and their applications for dual modal imaging and therapy of cancer cells. After the introduction of Gd(III) ions and cancer-targeting antibodies onto the surfaces of the hollow gold nanoparticles, they were successfully applied as both MRI and optical imaging contrast enhancers of cancer cells. The paramagnetic hollow gold nanoparticles were also successfully tested as a novel anti-cancer therapeutic agent, based on photothermal effects. The multifunctional hollow gold nanoparticles are also expected to be used for imaging specific cancer sites using MRI, and then for destroying cancer cells selectively *via* illumination with NIR light.

The authors acknowledge financial support from the Korea Science and Engineering Foundation (KOSEF), the KRIBB Research Initiative Program, and the Regional Technology Innovation Program of the Korean Government (MKE).

## Notes and references

1 (*a*) L. Levy, Y. Sahoo, K. S. Kim, E. J. Bergey and P. N. Prasad, *Chem. Mater*., 2002, **14**, 3715; (*b*) U. Hasegawa, S. I. M. Nomura, S. C. Kaul, T. Hirano and K. Akiyoshi, *Biochem. Biophys. Res. Commun*., 2005, **331**, 917.
2 (*a*) J. Kim, S. Park, J. E. Lee, S. M. Jin, J. H. Lee, I. S. Lee, I. Yang, J. S. Kim, S. K. Kim, M. H. Cho and T. Hyeon, *Angew. Chem., Int. Ed*., 2006, **45**, 7754; (*b*) T. A. Larson, J. Bankson, J. Aaron and K. Sokolov, *Nanotechnology*, 2007, **18**, 325101; (*c*) X. Ji, R. Shao, A. M. Elliott, R. J. Stafford, E. Esparza-Coss, J. A. Bankson, G. Liang, Z.-P. Luo, K. Park, J. T. Markert and C. Li, *J. Phys. Chem. C*, 2007, **111**, 6245.
3 (*a*) L. R. Hirsch, R. J. Stafford, J. A. Bankson, S. R. Sershen, B. Rivera, R. E. Price, J. D. Hazle, N. J. Halas and J. L. West, *Proc. Natl. Acad. Sci. U. S. A*., 2003, **100**, 13549; (*b*) X. Huang, I. H. El-Sayed, W. Qian and M. A. El-Sayed, *J. Am. Chem. Soc*., 2006, **128**, 2115; (*c*) V. P. Zharov, K. E. Mercer, E. N. Galitovskaya and M. S. Smeltzer, *Biophys. J*., 2006, **90**, 619.
4 (*a*) A. Bjørnerud and L. Johansson, *NMR Biomed*., 2004, **17**, 465; (*b*) B. Bonnemain, *J. Drug Target*., 1998, **6**, 167; (*c*) T. Neuberger, B. Schopf, H. Hofmann, M. Hofmann and B. Von Rechenberg, *J. Magn. Magn. Mater*., 2005, **293**, 483.
5 J. W. M. Bulte and D. L. Kraitchman, *NMR Biomed*., 2004, **17**, 484.
6 (*a*) G. A. F. Van Tilborg, W. J. M. Mulder, P. T. K. Chin, G. Storm, C. P. Reutelingsperger, K. Nicolay and G. J. Strijkers, *Bioconjugate Chem*., 2006, **17**, 865; (*b*) E. A. Anderson, S. Isaacman, D. S. Peabody, E. Y. Wang, J. W. Canary and K. Kirshenbaum, *Nano Lett*., 2006, **6**, 1160.
7 (*a*) J. V. Frangioni, *Curr. Opin. Chem. Biol*., 2003, **7**, 626; (*b*) R. Weissleder, *Nat. Biotechnol*., 2001, **19**, 316.
8 C. Loo, A. Lowery, N. Halas, J. West and R. Drezek, *Nano Lett*., 2005, **5**, 709.
9 J. M. Lee, H. K. Park, Y. Jung, J. K. Kim, S. O. Jung and B. H. Chung, *Anal. Chem*., 2007, **79**, 2680.
10 (*a*) J. Chen, B. Wiley, Z. Y. Li, D. Campbell, F. Saeki, H. Cang, L. Au, J. Lee, X. Li and Y. Xia, *Adv. Mater*., 2005, **17**, 2255; (*b*) J. Chen, J. M. McLellan, A. Siekkinen, Y. Xiong, Z. Y. Li and Y. Xia, *J. Am. Chem. Soc*., 2006, **128**, 14776.
11 (*a*) M. H. Falk and R. D. Issels, *Int. J. Hyperther*., 2001, **17**, 1; (*b*) B. Hildebrandt, P. Wust, O. Ahlers, A. Dieing, G. Sreenivasa, T. Kerner, R. Felix and H. Riess, *Crit. Rev. Oncol./Hematol*., 2002, **43**, 33.

 